Radiative and Conductive Transfer for a Gas/Soot Mixture Between Diffuse Parallel Plates

Theodore F. Smith,* Abdullah M. Al-Turki,† Ki-Hong Byun,† and Tai K. Kim†
The University of Iowa, Iowa City, Iowa

This study examines the interaction of conductive and radiative transfer for a radiatively participating medium contained between two infinite, isothermal, opaque, and diffuse plates. The nongray medium consists of absorbing gases of carbon dioxide and water vapor and soot particles. The soot volume fraction is introduced to describe the degree of participation of the soot in the radiant exchange process. Solutions for the medium-temperature distributions and wall heat fluxes were acquired by the finite analytic with radiation method. Results are reported to ascertain the influence of the soot volume fraction, plate separation distance, and surface emittances on the heat transfer between the plates. The soot radiation dominates the absorbing gas radiation and significantly reduces the heat transfer.

Nomenclature

a_α, a_ϵ = gas absorptivity and emissivity weighting factors
a_s = soot weighting factor
A_α, A_ϵ = mixture absorptivity and emissivity weighting factors
b_s = soot emissivity polynomial coefficients
B = parameter defined by Eq. (4)
C_s = soot-volume fraction coefficient
f_v = soot-volume fraction
GG = volume-to-volume total exchange areas
$\overrightarrow{GG}, \overrightarrow{GS}$ = volume-to-volume and volume-to-surface directed flux areas
J_s = number of soot temperature polynomials
k = thermal conductivity, W/m-K
L = plate spacing, m
M = number of volume zones
N_g, N_s = number of gray components for gas and soot
N = conduction-to-radiation parameter, $k\kappa_{T,u}/4\sigma T_u^3$
P = sum of partial pressures for absorbing gases, atm
q = heat flux, W/m^2
q_a = volumetric radiant energy absorbed, W/m^2
Q = dimensionless heat flux, $q/4\tau_u\sigma T_u^4$
Q_a' = dimensionless volumetric absorbed radiant energy, $q_a \Delta y/4\tau_u\sigma T_u^4$
Q^0 = dimensionless overall heat flux
S = dimensionless distance between zones, $\Delta y/L$
SG, SS = surface-to-volume and surface-to-surface total exchange areas
$\overrightarrow{SG}, \overrightarrow{SS}$ = surface-to-volume and surface-to-surface directed flux areas
T = temperature, K
y = spatial variable, m
ϵ = surface emittance
θ = dimensionless temperature, T/T_u
κ = mixture absorption coefficient, m^{-1}
κ_g = absorbing gas absorption coefficient, (atm-m)$^{-1}$
κ_s = soot absorption coefficient, m^{-1}
κ_T = mixture total absorption coefficient, m^{-1}
ρ = surface reflectance
σ = Stefan-Boltzmann constant, W/m^2-K^4
τ = optical thickness, $\kappa_T L$
$\boldsymbol{gg}$ = volume-to-volume direct exchange area matrix
$\boldsymbol{GG}$ = volume-to-volume total exchange area matrix
$\boldsymbol{I}$ = identity matrix
$\boldsymbol{R}$ = matrix defined by Eq. (8d)
$\boldsymbol{sg}, \boldsymbol{ss}$ = volume-to-surface and surface-to-surface direct exchange area matrix
$\boldsymbol{SG}, \boldsymbol{SS}$ = volume-to-surface and surface-to-surface total exchange area matrix

Subscripts

ℓ = lower plate
p = previous iteration temperature
u = upper plate

Received April 29, 1985; presented as Paper 85-1070 at the AIAA 20th Thermophysics Conference, Williamsburg, VA, June 19-21, 1985; revision received Dec. 23, 1985.

*Professor, Department of Mechanical Engineering. Member AIAA.
†Graduate Student, Department of Mechanical Engineering.

Introduction

THE simultaneous interaction of radiative and conductive transfer has received considerable attention, as indicated by the literature review reported by Viskanta.[1] For a plane layer system, the studies by Yuen,[2] Soufiani et al.,[3] and Gupta et al.[4] could be added. Although there have been numerous studies regarding techniques for evaluation of the radiant contribution, results are lacking that consider the simultaneous contribution of radiative and conductive transfer in a mixture composed of absorbing and emitting gases and absorbing and emitting soot particles. Reported studies have made the gray property assumption, have considered only one or two bands for an absorbing gas, or have examined only soot particles. Few studies have included reflecting boundaries. Since a plane layer system appears in several engineering systems and serves as a convenient geometry for examining trends, it is of interest to examine radiative and conductive transfer for a gas/soot mixture when the system boundaries are reflecting.

This study examines the simultaneous interaction of radiative and conductive transfer for a radiatively participating nongray medium contained between two infinite parallel plates separated a distance L, and maintained at uniform temperatures of T_ℓ and T_u. The medium is in local thermodynamic equilibrium and has a refractive index of unity. The medium is stationary, exhibits a constant thermal conductivity k, and contains an absorbing and emitting gas/soot mixture. In view of the expected soot concentration,[5] it is reasonable to assume that the medium thermal conductivity does not vary with the

soot concentration. For temperatures and soot particle sizes common to combustion systems, it can be assumed that scattering is negligible.[5] Thermal conduction normal to the plates is considered. The plates are opaque, gray, and diffuse emitters and reflectors of radiant energy with surface emittances of ϵ_ℓ and ϵ_u. Steady-state conditions prevail. One-dimensional temperature profiles for the medium exist normal to the plates as a result of these statements.

Analysis

Formulation

An energy balance on a differential slab of thickness dy within the medium states

$$k\frac{d^2T}{dy^2} = 4\kappa_T(T)\sigma T^4 - q_a \tag{1}$$

where T is the medium temperature at position y as measured normal to the plate at T_ℓ. The term on the left-hand side of Eq. (1) is the net conductive transfer into the slab. The first term on the right-hand side of Eq. (1) is the radiant emission with $\kappa_T(T)$ denoting the total absorption coefficient for the gas/soot mixture evaluated at T. q_a is the volumetric radiant absorption for the differential slab. Specific expressions for κ_T and q_a are cited later. The boundary conditions are

$$@y = 0, \quad T = T_\ell; \quad @y = L, \quad T = T_u \tag{2}$$

Solutions to Eq. (1) with boundary conditions stated by Eq. (2) were obtained using the finite analytic with radiation method (FARM) as reported by Smith and Severin.[6] In preparation for the solution scheme, the plane layer is divided into M volume zones of thickness Δy. For the present results, a uniform zonal spacing was selected since there did not appear to be an advantage to using nonuniform spacings.[6] The FARM involves linearization of the emission term within a zone and assumes that the radiant absorption term is constant within that zone. An analytical solution to the linearized energy balance equation can then be obtained in terms of the adjacent zone temperatures. The analytical solution is then evaluated at the center of the considered zone. The resultant expression for the zone temperature is

$$\theta_i = \frac{1}{2\cosh B_i S}\left[\theta_{i-1} + \theta_{i+1} - \frac{2\tau_u Q^r_{a,i}}{\tau_i S \theta^3_{p,i}}(1 - \cosh B_i S)\right] \tag{3}$$

where $i = 2$ to $M-1$. Special forms for Eq. (3) must be derived for $i = 1$ and M where $i = 1$ represents the volume zone adjacent to the plane at T_ℓ. B_i is defined as

$$B_i = \left(\tau_i \tau_u \theta^3_{p,i}/\bar{N}\right)^{1/2} \tag{4}$$

Subscripts i and u denote that τ_i and τ_u are based on the ith zone temperature and the upper-plate temperature, respectively, in the evaluation of κ_T. For a gray analysis,[6] the product of $\tau_i\tau_u$ in the expression for B_i reduces to τ_0^2. For the nongray analysis τ_i is related to the zone emission, as in Eq. (1), and τ_u is introduced so that $\bar{N}$ appears. Since the solution does not yield explicitly the medium temperature, an iteration scheme must be employed. Thus θ_p, the previous iteration temperature, must be updated after each iteration. The FARM has been demonstrated to yield accurate and stable solutions.[6] The linearization of the emission term is applied to a local region. The entire nonlinear problem is solved, and the small temperature difference assumption is not invoked.

Radiant Absorption

From the zone analysis,[6] the volumetric absorbed radiant flux is evaluated from

$$Q^r_{a,i} = (1/4\tau_u)\left[\overrightarrow{S_\ell G_i}\theta^4_\ell + \overrightarrow{S_u G_i} + \sum_{j=1}^{M}\overrightarrow{G_j G_i}\theta^4_j\right] \tag{5}$$

where $\overrightarrow{SG}$ are surface to gas and $\overrightarrow{GG}$ are gas-to-gas directed flux areas for a gas/soot mixture

$$\overrightarrow{S_i G_j} = \sum_{n=1}^{N_s}\sum_{m=0}^{N_g} A_{\alpha,n,m}(T_i, T_j)(S_i G_j)_{n,m} \tag{6}$$

and

$$\overrightarrow{G_i G_j} = \sum_{n=1}^{N_s}\sum_{m=0}^{N_g} A_{\epsilon,n,m}(T_i)(G_i G_j)_{n,m} \tag{7}$$

N_s and N_g are the number of gray gas components corresponding to the soot and absorbing gases, respectively, for the weighted sum of the gray gases model. A_α and A_ϵ are the weighting factors for absorptivity and emissivity, respectively. Total exchange areas for surface-to-gas and gas-to-gas radiant exchanges are represented by SG and GG, respectively, for a mixture absorption coefficient $\kappa_{n,m}$.

Total Exchange Areas

Total exchange areas (TEA) account for both direct transport of radiant energy between zone pairs and indirect transport through multiple diffuse reflections from the surfaces. TEA depend on surface emittances and direct exchange areas (DEA) that are expressed in terms of an optical depth, defined as the product of mixture absorption coefficient and path length. For evaluation of DEA expressions see Ref. 6. The formulation for TEA in terms of emittance and DEA is based on the matrix method of Noble.[7] TEA are evaluated from the following matrix expressions in dimensionless form

$$\boldsymbol{SS} = \epsilon\boldsymbol{I}\cdot\boldsymbol{R}\cdot\boldsymbol{ss}\cdot\epsilon\boldsymbol{I} \qquad (2\times 2) \tag{8a}$$

$$\boldsymbol{SG} = \epsilon\boldsymbol{I}\cdot\boldsymbol{R}\cdot\boldsymbol{sg} = (\boldsymbol{GS})^T \qquad (2\times M) \tag{8b}$$

$$\boldsymbol{GG} = \boldsymbol{gg} + \boldsymbol{gs}\cdot\rho\boldsymbol{I}\cdot\boldsymbol{R}\cdot\boldsymbol{sg} \qquad (M\times M) \tag{8c}$$

$$\boldsymbol{R} = [\boldsymbol{I} - \boldsymbol{ss}\cdot\rho\boldsymbol{I}]^{-1} \qquad (2\times 2) \tag{8d}$$

where the factors in parentheses to the right denote the number of TEA for each radiant exchange pair. $\epsilon\boldsymbol{I}$ and $\rho\boldsymbol{I}$ represent surface emittance and reflectance diagonal matrices. $\boldsymbol{ss}$, $\boldsymbol{sg}$, $\boldsymbol{gs}$, and $\boldsymbol{gg}$ correspond to DEA for surface-to-surface, gas-to-surface, surface-to-gas, and gas-to-gas radiant exchanges. DEA and TEA must be evaluated for each gray gas component absorption coefficient of the gas/soot mixture. Superscript T in Eq. (8b) denotes the transposed matrix. DEA and TEA satisfy the reciprocity relation for radiant exchange between zone pairs.

Gas/Soot Properties

The weighted sum of the gray gases model was employed for the total emissivity and absorptivity of a gas/soot mixture. This model postulates that the total properties can be represented by the sum of gray gas emissivities weighted with a temperature dependent factor. The gas emissivity is expressed in terms of the product of a mixture absorption coefficient and a path length. The total properties for a gas-soot mixture are expressed in terms of weighting factors and absorption coefficients for the gas and soot acting individually.[8,9] The weighting factors are expressed by polynomials in temperatures where coefficients have been developed for soot[8] and absorbing gases.[10]

The total absorption coefficient is

$$\kappa_T(T) = \sum_{n=1}^{N_s} \sum_{m=0}^{N_g} \kappa_{n,m} A_{\epsilon,n,m}(T) \tag{9}$$

where the gas/soot mixture absorption coefficient $\kappa_{n,m}$ for the n, m gray gas component is evaluated from

$$\kappa_{n,m} = \kappa_{s,n} + P\kappa_{g,m} \tag{10}$$

The soot absorption coefficient for the nth gray gas component $\kappa_{s,n}$ is given by

$$\kappa_{s,n} = C_{s,n} f_v \tag{11}$$

where $C_{s,n}$ are the soot volume fraction coefficients. Values for $C_{s,n}$ are furnished in Table 1. A second soot coefficient was used in Ref. 9 and nearly has a value of unity. In the present study, this coefficient was assumed to be unity without any loss of accuracy. $\kappa_{g,m}$ is the gas absorption coefficient for the mth gray gas component with P denoting the sum of the partial pressures of the absorbing gases.

The mixture emissivity weighting factor is given by

$$A_{\epsilon,n,m}(T) = a_{s,n}(T)\, a_{\epsilon,m}(T) \tag{12}$$

and absorptivity by

$$A_{\alpha,n,m}(T, T_s) = a_{s,n}(T_s)\, a_{\alpha,m}(T, T_s) \tag{13}$$

where a_s are the soot weighting factors evaluated from temperature polynomial as follows:

$$a_{s,n} = \sum_{j=1}^{J_s} b_{s,n,j} T^{j-1} \tag{14}$$

Values for the soot emissivity polynomial coefficients are given in Table 1 for $J_s = 4$. No distinction needs to be made between emissivity and absorptivity weighting factors for the soot. T_s is the temperature of the zone where radiant energy originates from and irradiates the zone at T. a_ϵ and a_α are the gas emissivity and absorptivity weighting factors expressed by temperature polynomials. For the gas/soot mixture used in the present study $N_s = 2$ and $N_g = 3$, and there are eight mixture absorption coefficients including the clear gas component.

Wall Heat Flux

The conductive transfer at the lower plate is expressed by[6]

$$Q_\ell^c = -\left[\frac{\tau_1 \bar{N} \theta_{p,1}^3}{\tau_u^3}\right]^{1/2} \left[\frac{\theta_\ell \cosh x - \theta_2}{\sinh x} + \frac{\tau_u Q_{a,1}^r}{\tau_1 S \theta_{p,1}^3} \frac{(1-\cosh x)}{\sinh x}\right] \tag{15}$$

where $x = 3B_1 S/2$. A similar expression also applies for the conductive transfer at the upper plate. It should be noted that the conductive transfer depends on the radiant exchange as shown in Eq. (15). The dimensionless radiant energy leaving the lower plate is given by

$$Q_\ell^r = \frac{1}{4\tau_u}\left[\epsilon_\ell \theta_\ell^4 - \overrightarrow{S_\ell S_\ell}\theta_\ell^4 - \overrightarrow{S_u S_\ell} - \sum_{i=1}^{M} \overrightarrow{G_i S_\ell} \theta_i^4\right] \tag{16}$$

$\overrightarrow{SS}$ and $\overrightarrow{GS}$ denote the direct flux areas for surface-to-surface and gas-to-surface radiant exchanges, respectively, and are expressed

$$\overrightarrow{S_i S_j} = \sum_{n=1}^{N_s} \sum_{m=0}^{N_g} A_{\alpha,n,m}(T_i, T_j)(S_i S_j)_{n,m} \tag{17}$$

and

$$\overrightarrow{G_i S_j} = \sum_{n=1}^{N_s} \sum_{m=0}^{N_g} A_{\epsilon,n,m}(T_i)(G_i S_j)_{n,m} \tag{18}$$

where SS and GS are total exchange areas for surface-to-surface and gas-to-surface radiant exchanges. A similar expression is applicable for the radiant flux at the upper plate. The overall heat transfer for a plate is the sum of the conductive and radiative heat fluxes.

Solution Scheme

A numerical solution was used for the zone temperatures, as stated by Eq. (3), and involved an iteration scheme. The iterative solution was considered converged when the relative difference of the zone temperatures between successive iterations was less than the error criterion of 1×10^{-5}. The number of zones and computational times depended on the degree of radiant participation of the medium and the plate emittance. For example, the number of zones was 41 for a high-plate emittance ($\epsilon = 1.0$) and between 81 and 161 for a low-plate emittance ($\epsilon = 0.1$). The requirement for a larger number of zones for the low-plate emittance cases was attributed to the steep temperature gradients near the plates. Computational times on a PRIME 9950 computer system were between 11 and 800 s with the larger times for the cases of a highly radiating medium and a low-plate emittance.

Results and Discussion

The mixture temperature profiles and wall heat fluxes depend on several governing parameters: the thermal conductivity, radiative properties of the mixture (including the total and partial pressures of the absorbing gases and the soot volume fraction), emittances and temperatures of the plates, and the separation distance. For results presented here, $k = 0.0763$ W/m-k, $T_\ell = 750$ K, $T_u = 1500$ K, total pressure is 1 atm, and the absorbing gases are water vapor and carbon dioxide with partial pressures equal to 0.1 atm. Values of the total absorption coefficient and the conduction/radiation parameter are provided in Table 2 as an aid to identify the degree of participation of the gases and soot in the radiant exchange process. The values shown for $f_v = 0.01$, 0.1, and 1×10^{-6} are for those gases independent of f_v. Values for $\bar{N}$ are given only

Table 1 Soot coefficients

Coefficient	$n=1$	$n=2$
$C_{s,n}$	1.00802×10^6	3.23520×10^6
$b_{sn,1}$	1.420	−0.420
$b_{sn,2}$	-0.77942×10^{-3}	0.77942×10^{-3}
$b_{sn,3}$	-0.38408×10^{-7}	0.38408×10^{-7}
$b_{sn,4}$	0.24166×10^{-10}	-0.24166×10^{-10}

Table 2 Total absorption coefficient and conduction/radiation parameter

T, K	$f_v \times 10^6$	k_T, m^{-1} Gases	Soot	Mixture	$\bar{N} \times 10^3$ Mixture
750	0.01	3.31	0.0140	3.33	
	0.10		0.14	3.45	
	1.00		1.40	4.71	
1500	0.01	1.24	0.0269	1.26	0.126
	0.10		0.26	1.51	0.150
	1.00		2.69	3.92	0.391

for the upper-plate temperature that appears in the definition of $\bar{N}$ and for a mixture. The magnitude of $\bar{N}$ indicates that radiation tends to dominate conduction. Emphasis is placed on examining the influence of soot volume fraction, plate emittances that are equal, and plate separation distance. Results are presented for limiting cases of pure soot (RS) and pure absorbing gases (RG) and for combined gas/soot mixture (RGS). In all cases, conduction is included.

Representative dimensionless temperatures for black plates separated by distances of 1 m are shown in Fig. 1 for $f_v = 0.01$, 0.1, and 1×10^{-6}. The RG results are the same for all three values of f_v. The curves display the typical characteristics found in other simultaneous radiative and conductive studies.[11] Pure conduction results would be represented by a straight line connecting the lower- and upper-plate temperatures of 0.5 and 1.0, respectively. Results including radiation differ significantly from the pure conduction results. For $f_v = 0.01 \times 10^{-6}$, the RGS results are described adequately by the RG results. However, when the soot concentration is increased to $f_v = 1 \times 10^{-6}$, the RGS results are predicted by the RS results. As f_v increases from 0.01 to 1×10^{-6}, the RS results vary from those for the almost pure radiation case to the radiation/conduction case. The pure radiation case would have a centerline temperature near $\theta = [(\theta_\ell^4 + \theta_u^4)/2]^{0.25} \approx 0.85$. RS results for smaller and larger values of f_v approach the pure conduction results since the soot mixture is becoming optically thin and thick, respectively.

The influence of plate separation distance on the mixture temperature distributions for black surfaces and $f_v = 0.1 \times 10^{-6}$ is displayed in Fig. 2 for $L = 0.01$, 0.1, and 1 m. These results approach the pure conduction values for only the smallest value of L. The RGS result for $L = 0.01$ m are not bracketed by the RG and RS results as they are for $L = 0.1$ and 1 m. Thus, at small values of L, it appears that the RG and RS results are additive to obtain the RGS results. At large lengths, the RS results approach the pure radiation results.

The dimensionless temperatures for $L = 0.1$ m and $f_v = 0.1 \times 10^{-6}$ in Fig. 3 illustrate the influence of plate emittance where $\epsilon = 0.1$, 0.5, and 1.0. Only results for the RGS cases are shown, as those for RG and RS exhibit similar trends. As the emittance decreases, the results approach those for pure radiation and the temperature gradients near the plates become steeper. The influence of emittance is rather uniform as ϵ varies from 0.1 to 1.0.

For a small value of emittance, that is $\epsilon = 0.1$, dimensionless temperature results are shown in Figs. 4 and 5 to illustrate the influence of soot volume fraction and separation distance. Findings similar to those of Figs. 1 and 2 are applicable to these results. Note that the RS results in Fig. 4 are similar to those for pure radiation except near the plates where the temperatures must approach the plate temperatures as a result of conductive transfer. Comparison of results between Figs. 2 and 5 demonstrates that radiation effects are reduced as the emittance decreases. For example, when $L = 0.01$ m, the radiative flux at the lower wall is approximately 99% of the wall flux for $\epsilon = 1.0$, and the flux reduces to 56% for $\epsilon = 0.1$. These results would have applications to the evaluation of gas thermal conductivities. The RG, RS, and RGS results are nearly indistinguishable in Fig. 5 when $L = 0.01$ m.

Representative dimensionless wall heat fluxes as a function of f_v are displayed in Fig. 6 for $L = 1$ m and $\epsilon = 0.1$, 0.5, and 1.0. The wall heat fluxes are normalized with that for radiant exchange between black plates in the absence of a radiatively participating medium, that is, $q_c = \sigma(T_u^4 - T_\ell^4)$. The RG results are represented by dotted lines and are independent of f_v. RS results are shown only for $\epsilon = 0.5$ and 1.0 and nearly attain the radiant exchange results for two infinite gray parallel plates as f_v decreases. RGS results are illustrated for all emittances. For $\epsilon = 0.1$, the overall flux is shown with the

Table 3 Wall heat fluxes

L, m	q^c/q_c[a]	q^r/q_c	q^0/q_c
0.01	0.0415	0.984	1.03
0.10	0.0175	0.930	0.947
1.00	0.0118	0.711	0.722

[a] $q_c = \sigma(T_u^4 - T_\ell^4)$

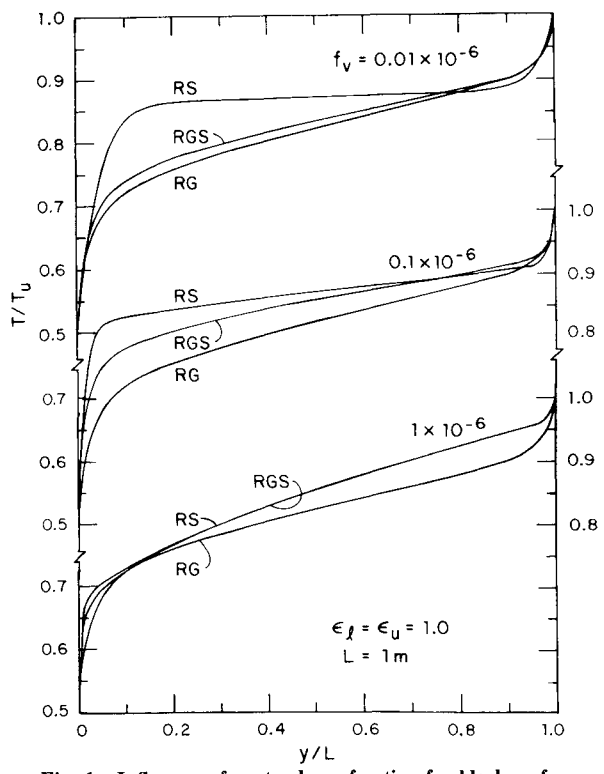

Fig. 1 Influence of soot volume fraction for black surfaces.

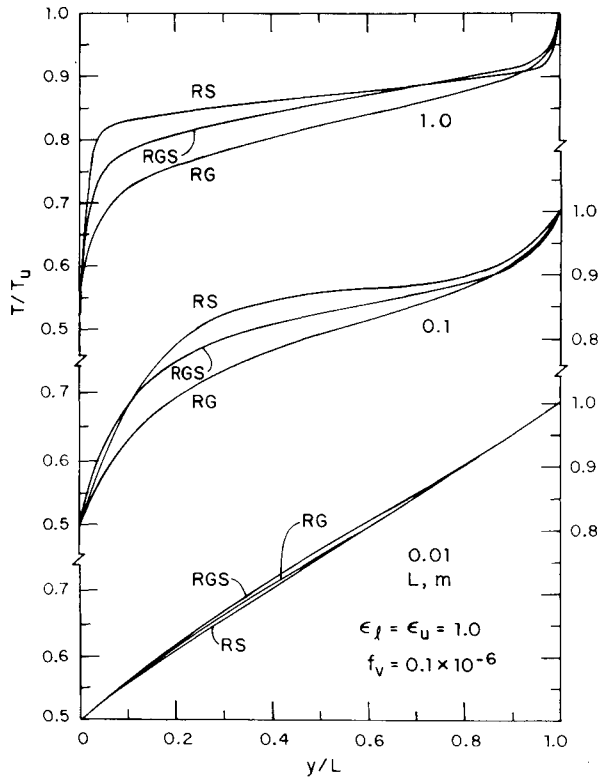

Fig. 2 Influence of separation distance.

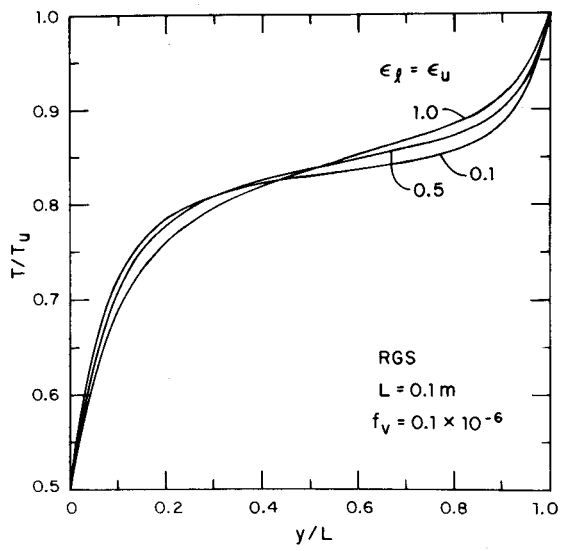

Fig. 3 Influence of emittance.

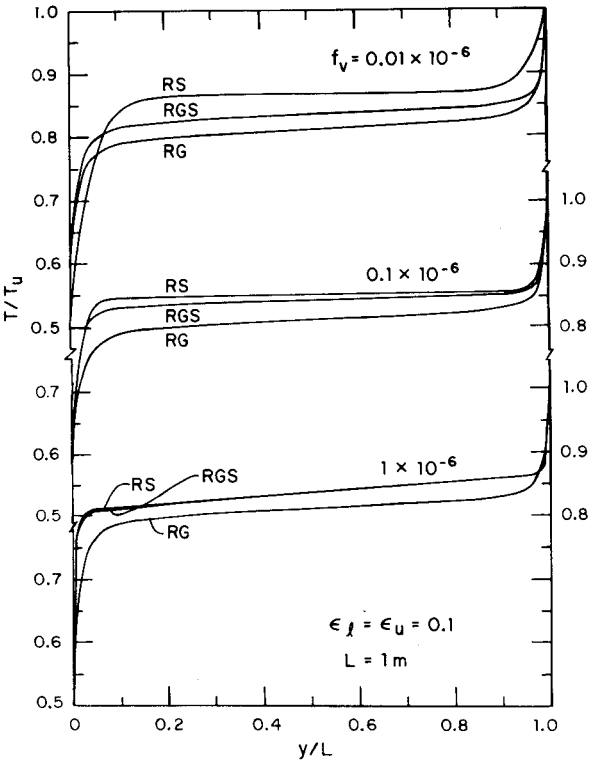

Fig. 4 Influence of soot volume fraction for low emittance.

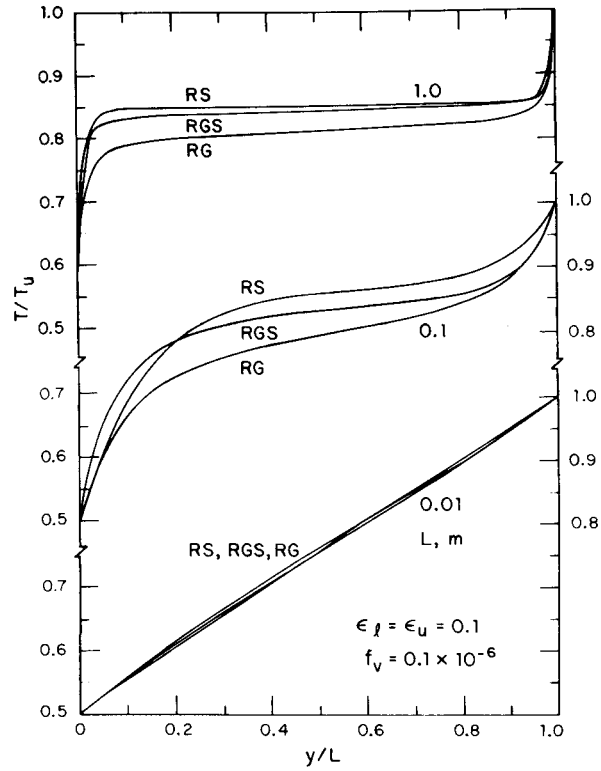

Fig. 5 Influence of separation distance.

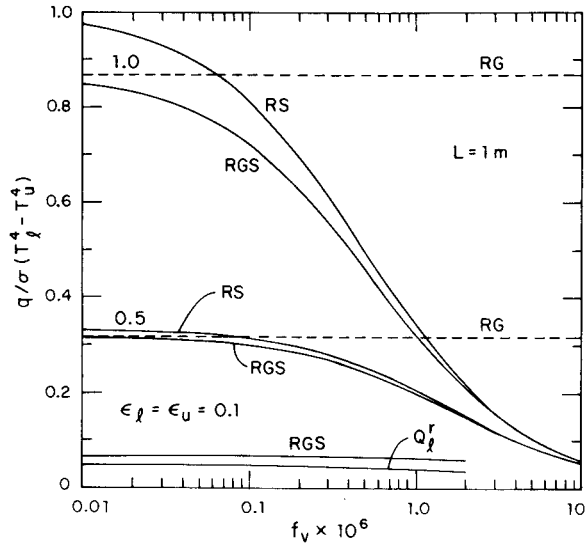

Fig. 6 Wall heat fluxes.

radiative flux at the lower plate. The difference between these two fluxes is the conductive flux. For the other values of ϵ, the conductive fluxes are less than 10% of the overall flux when $f_v < 1 \times 10^{-6}$. This percentage increases to about 15% for $f_v = 10 \times 10^{-6}$.

For $\epsilon = 0.1$, RS results, which exhibit a value of about 0.053 corresponding to a nonparticipating flux, are less than the RGS results. However, for the other values of ϵ, the RS results are greater than the RGS results shown in Fig. 6. As f_v increases all fluxes decrease, signifying a blockage of radiant exchange between the two plates, and approach the conductive fluxes since the medium becomes optically thick. Thus soot could be used as an effective shield between two surfaces.

The influence of separation distance on the wall heat fluxes is presented in Table 3 for $f_v = 0.1 \times 10^{-6}$ and $\epsilon = 1.0$. These fluxes are normalized with the factor of q_c. Conductive, radiative, and overall flux results are tabulated for $L = 0.01$, 0.1, and 1.0 m. As L decreases the conductive flux increases causing the overall flux to be greater than the radiant flux for a nonparticipating medium between black walls. Even for $L = 0.01$ m, the radiative flux represents about 96% of the overall flux.

Conclusions

An analysis determined temperature distributions and heat fluxes for simultaneous interaction of radiative and conductive transfer in a gas/soot mixture contained between two reflecting plates. The finite analytic with radiation method, in conjunction with the zonal analysis, was employed to obtain

results for several values of the governing parameters. The gas/soot radiative properties were furnished by the weighted sum of the gray gases model. Results illustrated that radiative transfer plays a dominant role in determining the mixture temperature profiles and wall heat fluxes. The influences of soot volume fraction, separation distance between the plates, and plate emittance were examined.

References

[1]Viskanta, R., "Radiation Heat Transfer: Interaction with Conduction and Convection and Approximate Methods in Radiation," *Proceedings of the 7th International Heat Transfer Conference*, Vol. 2, Hemisphere, New York, 1982, pp. 103-121.

[2]Yuen, W.W., "Radiative Heat Transfer Characteristics of a Soot/Gas Mixture," *Proceedings of the 7th International Heat Transfer Conference*, Vol. 2, Hemisphere, New York, 1982, pp. 577-582.

[3]Soufiani, A., Hartmann, J.M., and Taine, J., "Validity of Band-Model Calculations for C_2 and H_2 Applied to Radiative Properties and Conductive-Radiative Transfer," *Journal of Quantitative Spectroscopy and Radiative Transfer*, Vol. 33, March 1985, pp. 243-257.

[4]Gupta, R.P., Wall, T.F., and Truelove, J.S., "Radiative Scatter by Fly Ash in Pulverized-Coal Fired Furnaces: Application of the Monte Carlo Method to Anisotropic Scatter," *International Journal of Heat and Mass Transfer*, Vol. 26, November 1983, pp. 1649-1660.

[5]Siegel, R. and Howell, J.R., *Thermal Radiation Heat Transfer*, 2nd ed., McGraw-Hill, New York, 1981.

[6]Smith, T.F. and Severin, S.S., "Development of the Finite Analytic with Radiation Method," *Journal of Heat Transfer*, Vol. 107, November 1985, pp. 735-737.

[7]Noble, J.J., "The Zone Method: Explicit Matrix Relations for Total Exchange Areas," *International Journal of Heat Mass Transfer*, Vol. 18, February 1975, pp. 261-269.

[8]Alturki, A.M. and Smith, T.F., "Total Emissivity and Absorptivity of Gas-Soot Mixtures," Department of Mechanical Engineering, University of Iowa, Iowa City, Iowa, Tech. Rept. E-TFS-84-003, 1984.

[9]Felske, J.D. and Charalamopoulos, T.T., "Gray Gas Weighting Coefficient for Arbitrary Gas-Soot Mixtures," *International Journal of Heat Mass Transfer*, Vol. 25, December 1982, pp. 1849-1855.

[10]Smith, T.F., Shen, Z.F., and Friedman, J.N., "Evaluation of Coefficients for the Weighted Sum of Gray Gases Model," *Journal of Heat Transfer*, Vol. 104, November 1982, pp. 602-608.

[11]Ozisik, M.N., *Radiative Transfer*, Wiley, New York, 1973.